



SPECIAL ISSUE PAPER

Cu₂ZnSnS₄ solar cells with a single spin-coated absorber layer prepared via a simple sol-gel route

Na Kyoung Youn^{1,2}, Ganesh L. Agawane³, Dahyun Nam⁴, Jihye Gwak^{1,*},†, Seung Wook Shin³, Jin Hyeok Kim^{3,*},†, Jae Ho Yun¹, SeJin Ahn¹, Ara Cho¹, Young Ju Eo¹, Seung Kyu Ahn¹, Hyeonsik Cheong⁴, Dong Hwan Kim², Kee-Shik Shin¹ and Kyung Hoon Yoon¹

¹Photovoltaic Laboratory, Korea Institute of Energy Research, Daejeon, 305-343, Korea

²Department of Materials Science and Engineering, Korea University, Seoul, 136-701, Korea

³Department of Materials Science and Engineering, Chonnam National University, Gwangju, 500-757, Korea

⁴Department of Physics, Sogang University, Seoul, 121-743, Korea

SUMMARY

Carbon-free Cu₂ZnSnS₄ (CZTS) thin films were prepared via a simple spin-coating process based on a sol-gel precursor of methoxyethanol solution with metal salts and thiourea, followed by post-sulfurization. The sol-gel precursor solution was deposited onto molybdenum-coated glass substrates. The sulfurization process was carried out using a conventional furnace at 525 °C for 60 min in a nitrogen atmosphere with sulfur powder. The structural, morphological and compositional properties of as-sulfurized thin films were characterized using X-ray diffraction, Raman spectroscopy, scanning electron microscopy and Auger electron spectroscopy. Only a single coating of the precursor solution was applied to obtain uniform Zn-rich and Cu-poor CZTS films thicker than 1 μm after post-annealing. The best solar cell fabricated with the as-prepared CZTS films of band gap energy ~1.37 eV showed a short-circuit current density of 10.15 mA/cm², an open circuit voltage of 0.509 V, a fill factor of 33.72% and a conversion efficiency of 1.74%. Copyright © 2015 John Wiley & Sons, Ltd.

KEY WORDS

Cu₂ZnSnS₄; thin film solar cell; sol-gel process; single-coating; 2-methoxyethanol

Correspondence

*Jihye Gwak, Photovoltaic Laboratory, Korea Institute of Energy Research, Daejeon 305-343, Korea.

*Jin Hyeok Kim, Department of Materials Science and Engineering, Korea University, Seoul 136-701, Korea.

†E-mail: bleucoeur@kier.re.kr; jinhyeok@chonnam.ac.kr

Received 30 March 2015; Revised 11 September 2015; Accepted 6 October 2015

1. INTRODUCTION

Cu₂ZnSnS₄ (CZTS) quaternary semiconductor has recently emerged as a promising candidate for absorber layers in thin film solar cells because CZTS has a low cost, is less toxic, is made of abundant constituents, has optimal and direct band gap (~1.5 eV) and has high absorption coefficient (>10⁴ cm⁻¹), which are key factors for high conversion efficiency of thin film solar cells [1–8]. In 1988, Ito *et al.* reported the photovoltaic effect in CZTS compounds for the first time [9], and since then, research interest in CZTS solar cells has increased intensively because of the various advantages of the material. The solution-based process is very attractive for CZTS absorber preparation thanks to the cost and energy-saving potential for solar cell production. Furthermore, W. Wang *et al.* in 2013 reported that a world-record efficiency of 12.6% was achieved with a Cu₂ZnSn(S,Se)₄ (CZTSSe) solar cell using a hydrazine-based

approach [10]. However, hydrazine is a highly toxic and unstable compound that requires extreme caution for handling [11–14]. Thus, several research groups have investigated relatively safe non-vacuum processes for the CZTS thin film fabrication [12–14]. The use of binders, crack-avoiding agents and stabilizers such as terpineol, ethyl cellulose, oleylamine and monoethanolamine (MEA) has proven that superior-quality CZTS thin films can be prepared and applied in solar cells with promising performance [15–17]. However, these methods involve time-consuming and complicated nanoparticle-synthesis processes. Therefore, it is essential to investigate a simple, fast and eco-friendly, non-vacuum process to synthesize CZTS thin films.

Tanaka *et al.* introduced a simple sol-gel process for CZTS thin-film preparation using 2-methoxyethanol (2-ME) as a solvent [18]. They could even achieve 2.23%-conversion efficiency with a solar cell (active area=0.12 cm²) containing a CZTS absorber layer fabricated in 3% H₂S+N₂

atmosphere [18]. However, their coating and drying processes were repeated five times to obtain thick films because their sol was diluted by adding stabilizers such as MEA or ammonium acetate in deionized water [18,19]. Su *et al.* also prepared CZTS thin films using the sol-gel precursor solution containing Cu, Zn, Sn, S salts, 2-ME and MEA and showed that the thin films could work as solar cell absorber layers after post-sulfurization, reporting 5.1% conversion efficiency of the solar cell fabricated using a 1% Na doped CZTS thin film [20]. Lately, Kim *et al.* reported an 8.1%-efficient CZTS solar cell based on the 2-ME approach [21]. Though the authors showed the highest conversion efficiency among results from the 2-ME-based sol-gel approach by mixing polyvinylpyrrolidone in a Cu-Sn-S ink prior to adding a Zn precursor, they employed a complicated process including a long drying step because the organic compound polyvinylpyrrolidone easily produced unwanted carbon residue in the absorber layers. Furthermore, several depositions were necessary to obtain a desirable thickness of the CZTS absorber layers using the dilute sols of both Su *et al.* and Kim *et al.*

Park *et al.* prepared a homogeneous and compositionally uniform CZTS thin film by sol-gel process using 2-ME as a solvent without any stabilizer [22]. An excess amount of thiourea in the precursor solution was used to avoid the formation of secondary phases and sulfur (S) loss during post-annealing process, resulting in a homogeneous growth of CZTS films with the aid of formation of metal-S or metal-S-metal complexes [22,23]. They successfully made a Cu-poor and Zn-rich CZTS film based on single spin coating of the viscous sol-gel solution but did not show the performance of solar cells fabricated with as-prepared films.

A facile sol-gel process applied in this study based on a 2-ME solution of metal salts and thiourea does not require iterative spin-coating unlike the previous work [24], but only a single coating was needed to obtain the desirable thickness of nearly carbon free CZTS thin films after post-annealing of sulfurization using sulfur powder in a nitrogen atmosphere. Various characterizations were carried out on the as-deposited thin films after drying as well as post-annealing, and solar cells were also fabricated with single-layer coated CZTS absorbers to investigate the photovoltaic performance in this study.

2. EXPERIMENTAL AND DETAILS

$\text{Cu}_2\text{ZnSnS}_4$ precursor solutions were prepared by dissolving copper chloride (CuCl_2 1.6 M, 97% from Sigma Aldrich), zinc acetate ($\text{Zn}(\text{CH}_3\text{COO})_2$ 1.05–1.2 M, 99.99% from Sigma Aldrich), tin chloride (SnCl_2 0.8–0.95 M, 98% from Sigma Aldrich) and thiourea ($\text{SC}(\text{NH}_2)_2$ 6.4 M, 99.0% from Sigma Aldrich) into 20 mL of anhydrous 2-methoxyethanol ($\text{CH}_3\text{O}(\text{CH}_2)_2\text{OH}$, 99.8% from Sigma Aldrich). The composition of the precursor solutions was aimed at producing slightly Cu-poor and Zn-rich films. A colourless transparent sol was prepared with vigorous stirring at room temperature after adding thiourea in the metal precursor solution. This sol turned into a transparent yellow

sol over time and was aged for more than 1 month at room temperature before use in the sol-gel coating process.

A molybdenum (Mo) back contact layer $\sim 1 \mu\text{m}$ thick was deposited onto a soda lime glass substrate by direct current magnetron sputtering method using a 99.95% pure Mo target at room temperature (sheet resistance $\sim 0.2 \Omega/\text{sq}$). The as-prepared precursor solution was coated onto the Mo-sputtered substrates using a spin coater (ACE-200, Dong Ah Tech. Korea) at 2000 rpm for 20 sec. The coatings were dried at 120 °C, 200 °C and 300 °C for 4 h in air on a hot plate. Sulfurization was carried out in a furnace at 1.0237 atm using 0.5 g S powder in N_2 atmosphere for 120 °C-dried films. The sulfurization temperature and time were 445–575 °C and 60–100 min, respectively. After this annealing, the samples were cooled to room temperature in the furnace. Morphologies, crystal structures and compositional distributions of the as-annealed CZTS thin films were examined using field-emission scanning electron microscopy (FESEM, Hitachi S4700, Japan), grazing incidence X-ray diffraction (GIXRD, Rigaku Japan, D/MAX-2500 with a $\text{CuK}\alpha$ radiation source, $\lambda = 1.5406 \text{ \AA}$, at 40 kV, 100 mA, 5°/min of scan speed, 0.6° of grazing incidence angle) and Auger electron spectroscopy (AES, Perkin Elmer, SAM4300, using Ar gun ions at 3 kV for sputtering), respectively. Further, Raman scattering measurements were performed in the quasi-back scattering geometry by using the 514.5-nm line of an Ar ion laser, 632.8-nm line of a He-Ne laser and the 325-nm line of a He-Cd laser as the excitation sources, as detailed in a previous work [25].

Taking into account of material properties of CZTS in comparison with copper indium gallium selenide thin films and research performed by many other groups in terms of the fabrication [26–28], solar cell devices were fabricated by chemical bath deposition of a 60 nm CdS buffer layer on the as-prepared CZTS absorber layers, followed by the deposition of 50-nm-thick i-ZnO and 400-nm-thick aluminium (Al)-doped zinc oxide using radio frequency sputtering (sheet resistance $\sim 100 \Omega/\text{sq}$ and transmittance $\sim 88\%$). The metal contacts were made using thermally evaporated Al, resulting in a cell structure of soda lime glass/Mo/CZTS/CdS/ZnO/Al grid. The total area of the cell was 0.527 cm^2 . The conversion efficiency and the external quantum efficiency (EQE) for the completed solar cells were characterized using a class AAA solar simulator (WXS-155S-L2, WACOM, Japan) at an illumination of air mass 1.5 G with a total irradiance of $100 \text{ mW}/\text{cm}^2$ and an incident photon conversion efficiency measurement unit (PV Measurements, Inc., USA), respectively.

3. RESULTS AND DISCUSSION

Figure 1 shows cross-sectional scanning electron micrographs (SEM) of CZTS precursor films dried in air for 4 h at different temperatures: (i) 120 °C, (ii) 200 °C and (iii) 300 °C. Despite volume contraction during drying, the precursor films are highly uniform and crack-free with dense microstructures. The thickness of CZTS precursor

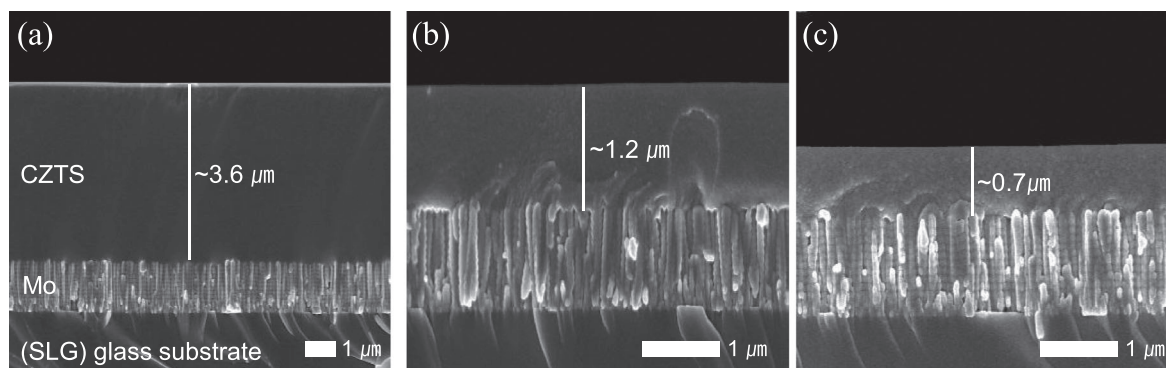


Figure 1. Cross-sectional scanning electron micrographs of dried precursor samples on Mo-coated glass substrates (a) 120 °C, (b) 200 °C and (c) 300 °C.

thin films decreases from 3.6 to 0.7 μm with increase in drying temperature from 120 °C to 300 °C. The reason for the decrease in thickness seems to be the evaporation of 2-ME and carbon-related residues at higher temperature. Similar behaviour has been reported in the literature [20].

GIXRD patterns of the CZTS precursor films dried at different temperatures of 120 °C, 200 °C and 300 °C are shown in Figure 2. The overall broad peaks indicate the existence of amorphous phases in these dried films. While the pattern for the 120 °C-dried sample shows only the amorphous phase in the film, peaks are detected at 28.5°, 47.4° and 56.3° corresponding to (112), (220) and (312) planes of the CZTS phase for 200 °C-dried and 300 °C-dried samples [29]. Similar X-ray diffraction (XRD) results for as-deposited thin films are reported in the literature [29]. Small peaks at 40.5° and 73.7° are attributed to the Mo cubic structure (JCPDS no. 42-1120) from the back contact layer.

Typical morphology and crystallographic data on the precursor films dried at 120 °C and then sulfurized at 525 °C for 1 h were obtained by SEM and XRD, respectively, as shown in Figure 3. Temperatures lower than 525 °C did not seem to be enough for the film grain growth, while films sulfurized at higher temperatures showed well-grown dense structure (cf. supporting

information). The 525 °C-sulfurized thin films have non-uniform surfaces with average grain size of ~ 200 nm (Figure 3(a)). The cross-sectional SEM image in Figure 3(b) shows that the sulfurized CZTS thin film is thicker than 2 μm , while a very porous microstructure is observed. This porous morphology seems attributed to the evaporation of organic residues from precursor films dried at 120 °C. The denser films after drying at higher temperatures shown in Figure 1 resulted in denser sulfurized absorber layers with better grain growth (not shown here), but it was difficult to obtain perfectly crack-free annealed films with those denser dried films. In Figure 3(c), the XRD pattern of the sulfurized film of Figure 3(a,b) exhibits major peaks at 23.1°, 28.5°, 33.0°, 47.4°, 56.3°, 69.2° and 76.4°, which correspond to (110), (112), (200), (220), (312), (008) and (332) planes of the kesterite CZTS compound (JCPDS no. 26-0575) [18,30,31]. There are no unidentified peaks in the XRD pattern of the sulfurized film. However, it is known that distinguishing the kesterite CZTS phase by analysing XRD patterns from secondary phases, such as tetragonal or cubic Cu_2SnS_3 (CTS) and cubic ZnS is difficult because their lattice constants are nearly identical [32,33]. Therefore, complementary analyses should be performed to verify the existence of such binary and ternary phases.

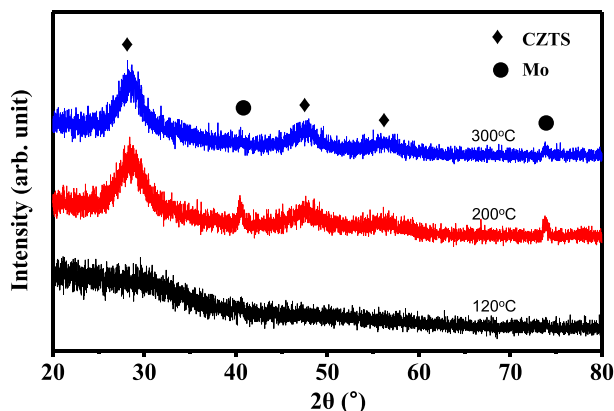


Figure 2. Comparison of the X-ray diffraction patterns of precursor thin films dried at different temperatures.

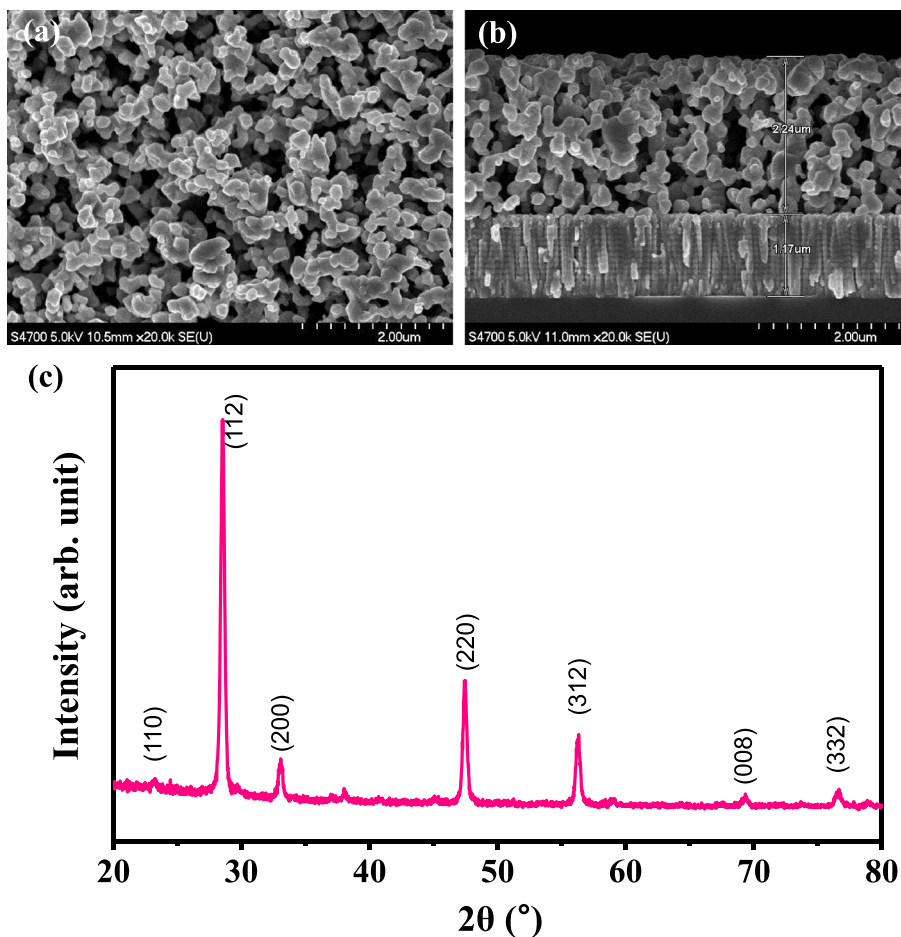


Figure 3. Surface, cross-sectional scanning electron micrographs and X-ray diffraction pattern of $\text{Cu}_2\text{ZnSnS}_4$ thin films sulfurized at 525°C for 1 h.

It is well known that the CZTS phase is detected by the presence of Raman peaks at 96 , 288 , 338 and 671 cm^{-1} when the Raman spectroscopy, which is a sensitive tool for phase identification, is equipped with a 514.5-nm line of an Ar ion laser [34]. However, different-wavelength lasers should be used for Raman spectroscopy to detect CTS or ZnS, which can exist in the sulfurized CZTS thin film as secondary phases because they cannot be clearly detected by the same laser source [35,36]. Using an UV-ranged laser source, detection sensibility to the presence of ZnS phase in the 525°C -sulfurized CZTS thin film could be enhanced in the Raman spectroscopy as presented in Figure 4. Low intensities of peaks located at 347 , 699 , 1044 and 1390 cm^{-1} , which are attributed to ZnS, are observed in the Raman spectrum from excitation by the 325-nm line of a He–Cd laser (Figure 4 (a)), similar to earlier reports [36], while the spectrum obtained using an Ar ion laser shows only peaks located at 288 , 338 and 671 cm^{-1} caused by pure kesterite CZTS (Figure 4(b)). A ternary impurity of the CTS phase, which might affect the optical properties of the absorber layer, was also detected in the sulfurized absorber by

the He–Ne laser-excitation in Raman spectroscopy, showing several peaks at 80 , 262 , 304 and 366 cm^{-1} in Figure 4(b) [32].

AES depth profiles of the CZTS absorber sulfurized at 525°C for 1 h after drying a film spin-coated with a precursor sol of a molar ratio of $\text{Cu}:\text{Zn}:\text{Sn}:\text{S} = 1.6:1.1:0.9:6.4$ are shown in Figure 5. Though the film showed a slight non-uniformity in the elemental composition, Cu-poor and Zn-rich stoichiometry was obtained throughout the film. Moreover, carbon residue was scarcely observed across the Cu-poor and Zn-rich absorber layer.

The current density–voltage (J - V) characteristic and EQE data of solar cells fabricated with the absorber layer in Figure 5 is presented in Figure 6. The best cell whose SEM cross-sectional image is in Figure 6(a) showed a conversion efficiency of 1.74% with an open-circuit voltage (V_{oc}) of 0.509 V , a short-circuit current (J_{sc}) of 10.15 mA/cm^2 and a fill factor (FF) of 33.72% (Figure 6(b)). Low J_{sc} and FF could be attributed to the porous absorber layer and the presence of trivial secondary phases, such as ZnS and CTS on the surface area of the CZTS layer as those secondary phases in the interfacial region can increase

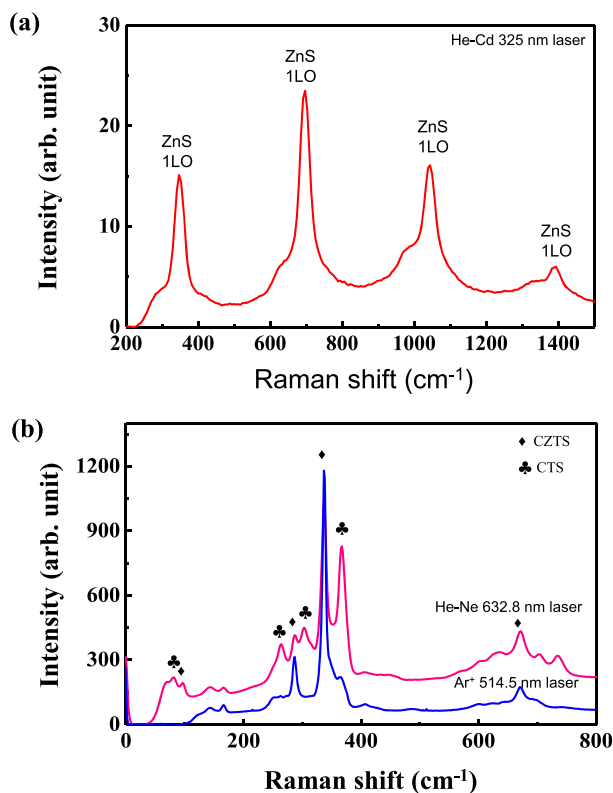


Figure 4. Raman spectra obtained for the sulfurized $\text{Cu}_2\text{ZnSnS}_4$ thin film: using (a) a UV-range laser source (325-nm line of a He-Cd laser) and (b) visible-range laser sources (514.5-nm line of an Ar^+ laser and 632.8-nm line of He-Ne laser).

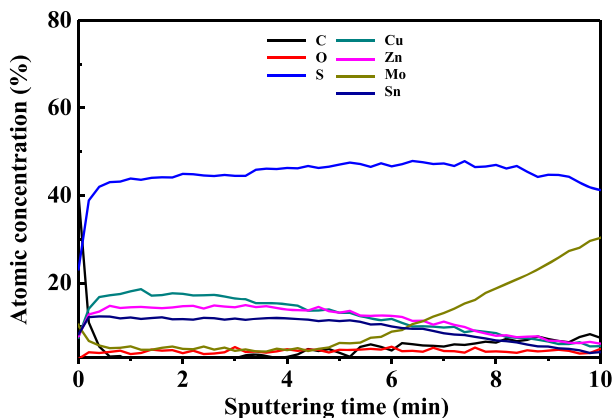


Figure 5. Auger electron spectroscopy depth profiles of the $\text{Cu}_2\text{ZnSnS}_4$ thin film sulfurized at 525°C for 1 h after drying a film spin-coated with a precursor sol of a molar ratio of $\text{Cu}:\text{Zn}:\text{Sn}:\text{S} = 1.6:1.1:0.9:6.4$.

recombination and shunt in the junction area of the solar cells, resulting in low EQE of the best cell at short wavelength shown in Figure 6(c) [37]. Strong loss in the CdS-edge ($\lambda \sim 450$ nm) seems related to the porous structure of CZTS absorber layer. As CdS buffer was infiltrated on the porous structure as shown in Figure 6(a) (and see 'supporting information' for EDS result), the buffer layer

could be thicker than expected and inhomogeneous on the absorber, resulting in low EQE at $\lambda \sim 450$ nm. Moreover, low EQE at longer wavelengths seems due to short carrier-diffusion lengths or insufficient penetration of the depletion range into absorber layer [37]. The optical band gap energy of the absorber determined by EQE in Figure 6 (c) is 1.37 eV, which is lower than the typically cited band

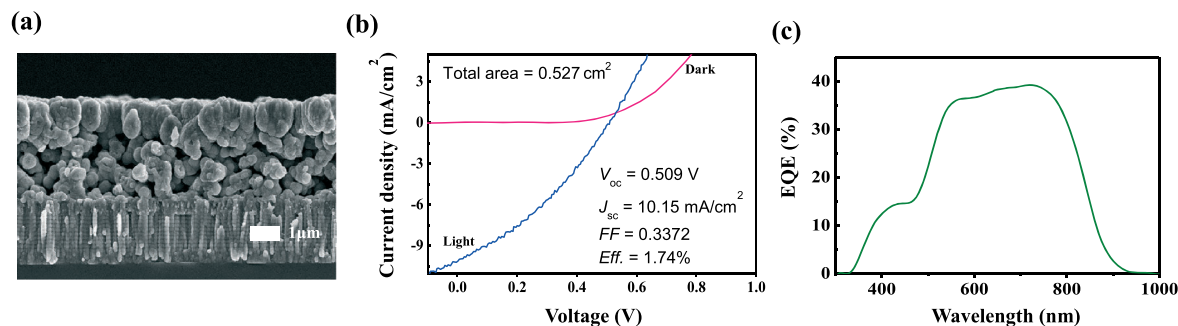


Figure 6. (a) Cross-sectional scanning electron micrograph, (b) Light and dark J - V curves and (c) external quantum efficiency curve of the 1.74% $\text{Cu}_2\text{ZnSnS}_4$ thin film solar cell.

gap energy of CZTS (1.45–1.5 eV). The presence of secondary CTS phase in the absorber layer, which shifts the optical absorption edge towards the lower energy, appears to be the reason for the low band gap energy of the fabricated CZTS absorber layer.

Solar cells fabricated with absorber layers sulfurized at different temperatures lower or higher than 525 °C in this study (see ‘supporting information’ for images of the absorber layers) did not perform better than the best cell, probably because of unreacted residues or undesired impurities formed, respectively. Further analyses and studies are going on to get higher quality of the absorber film through annealing optimization to obtain a higher conversion efficiency of CZTS solar cells.

4. CONCLUSIONS

Nearly carbon-free CZTS absorber layers were prepared via sulfurization of single spin-coated thin films deposited using a facile sol-gel technique. The best solar cell fabricated with a CZTS absorber layer produced a conversion efficiency of 1.74% despite a porous microstructure of the absorber layer as well as the existence of several secondary phases, such as CTS and ZnS. Further research on CZTS grain growth without secondary phases by optimizing the post-annealing process using another system such as rapid thermal process will improve the morphology of the absorber layer and photovoltaic cell performance.

ACKNOWLEDGEMENTS

This work was conducted under the framework of the Research and Development Program of the Korea Institute of Energy Research (KIER) (B5-2419), and by the International Collaborative Energy Technology R&D Program of the Korea Institute of Energy Technology Evaluation and Planning (KETEP), granted financial resource from the Ministry of Trade, Industry & Energy, Republic of Korea (No. 20138520011120). This work was also partly supported by the Center for Advanced Meta-Materials (CAMM) funded by the Ministry of Science, ICT and

Future Planning as Global Frontier Project (CAMM-No. 2014M3A6B3063703).

REFERENCES

- Scragg JJ, Dale PJ, Peter LM, Zoppi G, Forbes I. New routes to sustainable photovoltaics: evaluation of $\text{Cu}_2\text{ZnSnS}_4$ as an alternative absorber material. *Physica Status Solidi (b)* 2008; **245**:1772–1778.
- Wadia C, Alivisatos AP, Kammen DM. Materials availability expands the opportunity for large-scale photovoltaics deployment. *Environmental Science & Technology* 2009; **43**:2072–2077.
- Katagiri H, Jimbo K, Maw WS, Oishi K, Yamazaki M, Araki H, Takeuchi A. Development of CZTS-based thin film solar cells. *Thin Solid Films* 2009; **517**:2455–2460.
- Habas SE, Platt HAS, van Hest MFAM, Ginley DS. Low-cost inorganic solar cells: from ink to printed device. *Chemical Reviews* 2010; **110**:6571–6594.
- Todorov T, Mitzi DB. Direct liquid coating of chalcopyrite light-absorbing layers for photovoltaic devices. *European Journal of Inorganic Chemistry* 2010; **2010**:17–28.
- Hall SR, Szymański JT, Stewart JM. Kesterite, $\text{Cu}_2(\text{Zn,Fe})\text{SnS}_4$ and stannite, $\text{Cu}_2(\text{Fe,Zn})\text{SnS}_4$, structurally similar but distinct minerals. *The Canadian Mineralogist* 1978; **16**:131–137.
- Schorr S. Structural aspects of adamantite like multinary chalcogenides. *Thin Solid Films* 2007; **515**:5985–5991.
- Schorr S, H ebl HJ, Tovar JM. A neutron diffraction study of the stannite-kesterite solid solution series. *European Journal of Mineralogy* 2007; **19**:65–73.
- Ito K, Nakazawa T. Electrical and optical properties of stannite-type quaternary semiconductor thin films. *Japanese Journal of Applied Physics* 1988; **27**:2094–2097.
- Wang W, Winkler MT, Gunawan O, Gokmen T, Todorov TK, Zhu Y, Mitzi DB. Device characteristics

- of CZTSSe thin-film solar cells with 12.6% efficiency. *Advanced Energy Materials* 2014; **4**:1301465.
- Hussain SM, Frazier JM. Cellular toxicity of hydrazine in primary rat hepatocytes. *Toxicological Sciences* 2002; **69**:424–432.
 - Saha SK, Guchhait A, Pal AJ. $\text{Cu}_2\text{ZnSnS}_4$ (CZTS) nanoparticle based nontoxic and earth-abundant hybrid pn-junction solar cells. *Physical Chemistry Chemical Physics* 2012; **14**:8090–8096.
 - Woo K, Kim Y, Moon J. A non-toxic, solution-processed, earth abundant absorbing layer for thin-film solar cells. *Energy & Environmental Science* 2012; **5**:5340–5345.
 - Ki W, Hillhouse HW. Earth-abundant element photovoltaics directly from soluble precursors with high yield using a non-toxic solvent. *Advanced Energy Materials* 2011; **1**:732–735.
 - Zhao W, Wang G, Tian Q, Yang Y, Huang L, Pan D. Fabrication of $\text{Cu}_2\text{ZnSn}(\text{S},\text{Se})_4$ solar cells via an ethanol-based sol-gel route using SnS_2 as Sn source. *ACS Applied Materials & Interfaces* 2014; **6**:12650–12655.
 - Cho JW, Ismail A, Park SJ, Kim W, Yoon S, Min BK. Synthesis of $\text{Cu}_2\text{ZnSnS}_4$ thin films by a precursor solution paste for thin film solar cell applications. *ACS Applied Materials & Interfaces* 2013; **5**:4162–4165.
 - Wang C-L, Manthiram A. Low-cost CZTSSe solar cells fabricated with low band gap CZTSe nanocrystals, environmentally friendly binder, and nonvacuum processes. *ACS Sustainable Chemistry & Engineering* 2014; **2**:561–568.
 - Tanaka K, Moritake N, Uchiki H. Preparation of $\text{Cu}_2\text{ZnSnS}_4$ thin films by sulfurizing sol-gel deposited precursors. *Solar Energy Materials & Solar Cells* 2007; **91**:1199–1201.
 - Maeda K, Tanaka K, Fukui Y, Uchiki H. Influence of H_2S concentration on the properties of $\text{Cu}_2\text{ZnSnS}_4$ thin films and solar cells prepared by sol-gel sulfurization. *Solar Energy Materials & Solar Cells* 2011; **95**:2855–2860.
 - Su Z, Sun K, Han Z, Cui H, Liu F, Lai Y, Li J, Hao X, Liu Y, Green MA. Fabrication of $\text{Cu}_2\text{ZnSnS}_4$ solar cells with 5.1% efficiency via thermal decomposition and reaction using a non-toxic sol-gel route. *Journal of Materials Chemistry A* 2014; **2**:500–509.
 - Kim K, Kim I, Oh Y, Lee D, Woo K, Jeong S, Moon J. Influence of precursor type on non-toxic hybrid inks for high-efficiency $\text{Cu}_2\text{ZnSnS}_4$ thin-film solar cells. *Green Chemistry* 2014; **16**:4323–4332.
 - Park H, Hwang Y, Bae B. Sol-gel processed $\text{Cu}_2\text{ZnSnS}_4$ thin films for a photovoltaic absorber layer without sulfurization. *Journal of Sol-gel Science and Technology* 2013; **65**:23–27.
 - Yeh MY, Lee CC, Wu DS. Influences of synthesizing temperatures on the properties of $\text{Cu}_2\text{ZnSnS}_4$ prepared by sol-gel spin-coated deposition. *Journal of Sol-gel Science and Technology* 2009; **52**:65–68.
 - Agawane GL, Shin SW, Vanalakar SA, Suryawanshi MP, Moholkar AV, Yun JH, Gwak J, Kim JH. Synthesis of simple, low cost and benign sol-gel $\text{Cu}_2\text{ZnSnS}_4$ thin films: influence of different annealing atmospheres. *Journal of materials science: Materials in electronics* 2015; **26**:1900–1907.
 - Park D, Nam D, Jung S, Ahn S, Gwak J, Yoon K, Yun JH, Cheong H. Optical characterization of $\text{Cu}_2\text{ZnSnSe}_4$ grown by thermal co-evaporation. *Thin Solid Films* 2011; **519**:7386–7389.
 - Delbos S. Kesterite thin films for photovoltaics: a review. *EPJ Photovoltaics* 2012; **3**:35004.
 - Jiang M, Yan X. $\text{Cu}_2\text{ZnSnS}_4$ Thin Film Solar Cells: Present Status and Future Prospects. In *In Solar Cells – Research and Application Perspectives*, Morales-Acevedo A (ed.). InTech: Rijeka, Croatia, 2013; 107–143.
 - Nagoya A, Asahi R, Kresse G. First-principles study of $\text{Cu}_2\text{ZnSnS}_4$ and the related band offsets for photovoltaic applications. *Journal of Physics: Condensed Matter* 2011; **23**:404203.
 - Yu X, Ren A, Wang F, Wang C, Zhang J, Wang W, Wu L, Li W, Zeng G, Feng L. Synthesis and characterization of CZTS thin films by sol-gel method without sulfurization. *International Journal of Photoenergy* 2014; **2014**:861249.
 - Lin X, Kavalakkatt J, Kornhuber K, Levchenko S, Lux-Steiner MCH, Ennaoui A. Structural and optical properties of $\text{Cu}_2\text{ZnSnS}_4$ thin film absorbers from ZnS and Cu_3SnS_4 nanoparticle precursors. *Thin Solid Films* 2013; **535**:10–13.
 - Zhou YL, Zhou WH, Du YF, Li M, Wu SX. Sphere-like kesterite $\text{Cu}_2\text{ZnSnS}_4$ nanoparticles synthesized by a facile solvothermal method. *Materials Letters* 2011; **65**:1535–1537.
 - Fernandes PA, Salomé PMP, da Cunha AF. Study of polycrystalline $\text{Cu}_2\text{ZnSnS}_4$ films by Raman scattering. *Journal of Alloys and Compounds* 2011; **509**:7600–7606.
 - Agawane GL, Shin SW, Vanalakar SA, Moholkar AV, Kim JH. Next generation promising $\text{Cu}_2(\text{Zn}_x\text{Fe}_{1-x})\text{SnS}_4$ photovoltaic absorber material prepared by pulsed laser deposition technique. *Materials Letters* 2014; **137**:147–149.
 - Fontané X, Izquierdo-Roca V, Saucedo E, Schorr S, Yuhymchuk VO, Valakh MY, Pérez-Rodríguez A, Morent JR. Vibrational properties of stannite and kesterite type compounds: Raman scattering analysis of $\text{Cu}_2(\text{Fe},\text{Zn})\text{S}_4$. *Journal of Alloys and Compounds* 2011; **539**:190–194.

35. He J, Sun L, Zhang K, Wang W, Jiang J, Chen Y, Yang P, Chu J. Effect of post sulfurization on the composition, structure and optical properties of $\text{Cu}_2\text{ZnSnS}_4$ thin films deposited by sputtering from a single quaternary target. *Applied Surface Science* 2013; **264**:133–138.
36. Fontané X, Calvo-Barrio L, Izquierdo-Roca V, Saucedo E, Pérez-Rodríguez A, Morente JR, Berg DM, Dale PJ, Siebentritt S. In-depth resolved Raman scattering analysis for the identification of secondary phases: characterization of $\text{Cu}_2\text{ZnSnS}_4$ layers for solar cell applications. *Applied Physics Letters* 2011; **98**:181905.
37. Cui H, Liu X, Song N, Li N, Liu F, Hao X. Impact of rapid thermal annealing of Mo coated soda lime glass substrate on device performance of evaporated $\text{Cu}_2\text{ZnSnS}_4$ thin film solar cells. *Materials Letters* 2014; **125**:40–43.

SUPPORTING INFORMATION

Additional supporting information may be found in the online version of this article at publisher's website.